

Document downloaded from:

<http://hdl.handle.net/10251/153775>

This paper must be cited as:

Dietrich, D.; Pang, L.; Kobayashi, A.; Fozard, JA.; Boudolf, V.; Bhosale, R.; Nguyen, T.... (2017). Root hydrotropism is controlled via a cortex-specific growth mechanism. *Nature Plants (Online)*. 3(6):1-8. <https://doi.org/10.1038/nplants.2017.57>



The final publication is available at

<https://doi.org/10.1038/nplants.2017.57>

Copyright Nature Publishing Group

Additional Information

1 **Abscisic acid controls root hydrotropism**
2 **via a cortex-specific growth regulatory mechanism**

3
4 Daniela Dietrich^{1,2*}, Lei Pang^{3*}, Akie Kobayashi^{3*}, John A. Fozard^{1,†}, Véronique Boudolf^{4,5},
5 Rahul Bhosale^{1,2,4,5}, Regina Antoni^{1,†}, Tuan Nguyen^{1,6}, Sotaro Hiratsuka³, Nobuharu Fujii³,
6 Yutaka Miyazawa⁷, Tae-Woong Bae³, Darren M. Wells^{1,2}, Markus R. Owen^{1,8}, Leah R.
7 Band^{1,8}, Rosemary J. Dyson⁹, Oliver E. Jensen^{1,10}, John R. King^{1,8}, Saoirse R. Tracy^{1,11,†},
8 Craig J. Sturrock^{1,11}, Sacha J. Mooney^{1,11}, Jeremy A. Roberts^{1,2}, Rishikesh P. Bhalerao^{12,13},
9 José R. Dinneny¹⁴, Pedro L. Rodriguez¹⁵, Akira Nagatani¹⁶, Yoichiroh Hosokawa¹⁷, Tobias I.
10 Baskin^{1,18}, Tony P. Pridmore^{1,6}, Lieven De Veylder^{4,5}, Hideyuki Takahashi^{3##} and Malcolm J.
11 Bennett^{1,2##}

12

13 ¹Centre for Plant Integrative Biology, University of Nottingham, Nottingham, LE12 5RD, UK
14 ²Plant & Crop Sciences, School of Biosciences, University of Nottingham, Nottingham, LE12 5RD, UK
15 ³Graduate School of Life Sciences, Tohoku University, Sendai 980-8577, Japan
16 ⁴Department of Plant Systems Biology, VIB, B-9052 Gent, Belgium
17 ⁵Department of Plant Biotechnology and Bioinformatics, Ghent University, B-9052 Gent, Belgium
18 ⁶School of Computer Science, University of Nottingham, Nottingham, NG8 1BB, UK
19 ⁷Faculty of Science, Yamagata University, Yamagata 990-8560, Japan
20 ⁸Centre for Mathematical Medicine & Biology, University of Nottingham, Nottingham, NG7 2RD, UK
21 ⁹School of Mathematics, University of Birmingham, Birmingham, B15 2TT, UK
22 ¹⁰School of Mathematics, University of Manchester, Oxford Road, Manchester, M13 9PL, UK
23 ¹¹Agricultural and Environmental Sciences, School of Biosciences, University of Nottingham,
24 Nottingham, LE12 5RD, UK
25 ¹²Department of Forest Genetics and Plant Physiology, SLU, S-901 83 Umea, Sweden
26 ¹³College of Science, KSU, Riyadh, Saudi Arabia
27 ¹⁴Carnegie Institution for Science, Department of Plant Biology, 260 Panama Street, Stanford, CA
28 94305, USA
29 ¹⁵Instituto de Biología Molecular y Celular de Plantas, Consejo Superior de Investigaciones
30 Científicas-Universidad Politécnica de Valencia, ES-46022 Valencia, Spain
31 ¹⁶Graduate School of Science, Kyoto University, Kyoto 606-8502, Japan
32 ¹⁷ Graduate School of Materials Science, Nara Institute of Science & Technology, Ikoma 630-0101,
33 Japan
34 ¹⁸Biology Department, University of Massachusetts, Amherst, Massachusetts, USA
35 † Present address: Computational and Systems Biology, John Innes Centre, Norwich NR4 7UH, UK
36 (J.A.F.); Centre Nacional d'Anàlisi Genòmica (CNAG-CRG) 08028 Barcelona, Spain (R.A.); School of
37 Agriculture and Food Science, University College Dublin, Belfield Campus, Dublin 4, Ireland (S.R.T.)
38 *Denotes equal contribution of authors
39 #Denotes co-corresponding authorship
40 *e-mail: malcolm.bennett@nottingham.ac.uk (M.J.B.); hideyuki@ige.tohoku.ac.jp (H.T.)

41 Plants can acclimate by using tropisms to link the direction of growth to
42 environmental conditions. Hydrotropism allows roots to forage for water, a process
43 known to depend on abscisic acid (ABA) but whose molecular and cellular basis
44 remains unclear. Here, we show that hydrotropism still occurs in roots after laser
45 ablation removed the meristem and root cap. Additionally, targeted expression
46 studies revealed hydrotropism depends on the ABA signalling kinase, SnRK2.2, and
47 **the hydrotropism-specific MIZ1 both acting** in elongation zone cortical cells.
48 Conversely, hydrotropism is inhibited by preventing differential cell-length increases
49 in the cortex, but not in other cell types. The cortex surrounds the endodermis, the
50 major site of ABA accumulation in roots, and might function like a 'perimeter fence',
51 sensing lateral movement of ABA. **We hypothesize that differential water movement**
52 **could induce a hormone response gradient that reorients root growth direction**
53 **towards a water source.**

54

55 Tropic responses represent important differential growth mechanisms roots employ to
56 explore their surrounding soil environment efficiently. In general, a tropic response can be
57 divided into several steps, comprising perception, signal transduction, and differential
58 growth. All of these steps have been well characterized for gravitropism, where gravity
59 sensing cells in the columella of the root cap generate a lateral auxin gradient, whilst
60 adjacent lateral root cap cells transport auxin to epidermal cells in the elongation zone,
61 thereby triggering the differential growth that drives bending¹⁻⁴. In gravi-stimulated roots, the
62 lateral auxin gradient is transported principally by AUX1 and PIN carriers³⁻⁵.

63 Compared with gravitropism, the tropic response to asymmetric water availability, i.e.,
64 hydrotropism, has been far less studied. **Previously, it was reported that** surgical removal
65 and ablation of the root cap reduces hydrotropic bending in pea⁶⁻⁸ and *A. thaliana* roots⁹,
66 suggesting that the machinery for sensing moisture gradients resides in the root cap. It has
67 also been reported that hydrotropic bending occurs due to differential growth in the
68 elongation zone^{7,10}. However unlike gravitropism, hydrotropism in *A. thaliana* is independent
69 of AUX1 and PIN-mediated auxin transport^{11,12}. Indeed, roots bend hydrotropically in the
70 absence of any redistribution of auxin detectable by auxin-responsive reporters^{13,14}. Instead,
71 root hydrotropism requires signalling by the hormone abscisic acid (ABA)¹². These findings
72 imply that, compared to gravitropism, hydrotropism requires a distinct signalling mechanism.

73 The involvement of ABA in hydrotropism was initially suggested by aberrant responses in
74 *A. thaliana* mutants deficient for ABA synthesis or response¹². More recently, loss-of-function
75 ABA receptor and response mutants that are insensitive or hypersensitive to ABA have been
76 shown to be insensitive and hypersensitive to a hydrotropic stimulus, respectively¹⁵. In
77 addition, hydrotropism in *A. thaliana* roots requires a gene called *MIZU-KUSSE1* (*MIZ1*)¹⁶,
78 **which is upregulated by application of 10 μ M ABA**¹⁷. Despite *miz1* roots being oblivious to
79 water potential gradients, they nevertheless bend like wild type in response to gravity¹⁶. The
80 *MIZ1* sequence contains a DUF617 domain that is conserved among the genomes of
81 terrestrial plants, but absent in algae and animals, suggesting a role for hydrotropism in the

82 evolution of land plants¹⁶. A functional *MIZ1:MIZ1-GFP* fusion protein is expressed in lateral
83 root cap cells as well as cortex and epidermis cells in the meristem and elongation zone^{17,18}.
84 However it is unclear whether this broad expression pattern is necessary for MIZ1's function
85 in hydrotropism or whether ABA signal transduction components have to be expressed in
86 specific root tip tissues for a hydrotropic response. The present study describes a series of
87 experiments in *A. thaliana* designed to identify the root tissues essential for a hydrotropic
88 response. We report that MIZ1 and a key ABA signal-transduction component SnRK2.2
89 expressed specifically in the root cortex are sufficient to drive hydrotropism, and conversely
90 that hydrotropism is blocked by inhibiting the ability of specifically the cortex to execute a
91 differential growth response. Our results support a re-evaluation of hydrotropic signalling,
92 revealing the importance of the cortex and the elongation zone for signal perception as well
93 as bending.

94

95 **Results**

96 ***The root meristem and columella are dispensable for hydrotropism***

97 To uncover which root cell types and zones are required during a hydrotropic response in *A.*
98 *thaliana* roots, we ablated cells using a femtosecond laser. Successful ablation of the
99 columella cells was confirmed by propidium iodide staining of root tissues (Fig. 1a, b) and
100 hydro- and gravitropism assays performed as described previously^{11,16} (for details on
101 hydrotropism assays, see also Supplementary Fig. 1). Whilst columella ablation successfully
102 inhibited the gravitropic response as previously reported¹, it did not inhibit the hydrotropic
103 response (Fig. 1c, e). Furthermore, the ablated roots elongated at an equivalent rate as the
104 intact roots throughout both gravitropism and hydrotropism assays (Fig. 1d, f). Even when
105 the ablation encompassed essentially the entire meristem, hydrotropism was scarcely
106 affected (Supplementary Fig. 2). **When seedlings with ablated root cap or meristem were**
107 **placed in an assay system that lacked the moisture gradient, ablated roots responded in the**

108 same way as intact roots, with only minimal bending, which showed that laser ablation does
109 not lead to unspecific, wounding associated bending responses (Supplementary Fig. 2).
110 Because previous experiments with laser ablation implicated the columella⁹, the experiments
111 were repeated in the split agar-sorbitol system, with manual excision of the distal region of
112 the root tip (~250 µm). In this system, control root tips bend 30° or more by 10 hours after
113 transfer, but do not bend detectably when the lower medium lacks sorbitol (Fig. 2b). As with
114 laser ablation, hydrotropic bending, though more variable, was unaffected on average in
115 roots without a columella and meristem and only happened in response to a water potential
116 gradient (Supplementary Fig. 2). We suggest the discrepancy arises from the earlier
117 experiments having been run under adverse conditions as indicated by the roots in the
118 previous report growing more than an order of magnitude more slowly than those used here.
119 We conclude that water potential gradients are sensed as well as responded to within the
120 elongation zone.

121

122 ***Root hydrotropism depends on the ABA signalling component SnRK2.2***ABA

123 represents a critical signal for numerous plant abiotic stress responses¹⁹ including root
124 hydrotropism. ABA responses are mediated by a negative regulatory signalling module
125 involving soluble receptors of the START-domain superfamily (PYR/PYL/RCARs), clade A
126 type 2C protein phosphatases (PP2Cs) and subclass III Snf1-related kinases (SnRK2s)¹⁹.
127 ABA binds to PYR1/PYL/RCAR, which induces a conformational change that allows the
128 receptor proteins to bind to, and thereby inhibit, PP2Cs^{20,21}. PP2Cs dephosphorylate
129 SnRK2s, suppressing their activity; thus SnRK2 activity increases in the presence of ABA
130 due to PP2Cs being bound to the PYR1/PYL/RCAR ABA receptors²². When active, the
131 SnRK2s phosphorylate transcription factors and other downstream targets^{19,22}.

132 To investigate how ABA controls hydrotropism, we characterised a double mutant
133 lacking the ABA signalling kinases SnRK2.2 and SnRK2.3²³. Although retaining some ABA
134 responsiveness, this double mutant was selected for experiments because, in contrast to
135 most mutants in ABA perception, it is neither dwarfed nor wilted. We initially assayed

136 hydrotropism in a split agar-based system. Hydrotropism in the *snrk2.2 snrk2.3* double
137 mutant was strongly attenuated, but was restored in the *snrk2.2 snrk2.3* double mutant
138 expressing the *SnRK2.2* gene under the control of its own promoter (Fig. 2b). Identical
139 results were obtained using a moisture gradient in air hydrotropic assay (Supplementary Fig.
140 5). Hence, the SnRK2.2 kinase appears to be required for hydrotropism.

141 As the *snrk2.2 snrk2.3* double mutant had slightly shorter roots and a reduced growth
142 rate compared to wild type (Supplementary Fig. 3), we compared the growth rates of the
143 double mutant on half strength Murashige and Skoog (MS) medium and hydrotropism plates
144 and found them to be comparable (Supplementary Fig. 3), ruling out hypersensitivity of the
145 *snrk2.2 snrk2.3* double mutant to sorbitol. In addition, we performed split agar hydrotropism
146 assays with younger wild type seedlings to assess whether a reduction in tip angle was
147 caused simply by a reduced root growth rate. Roots bent with similar kinetics despite
148 differences in length and growth rate, indicating that hydrotropic bending is not proportional
149 to root growth rate (Supplementary Fig. 3).

150

151 ***Hydrotropism requires SnRK2.2 signalling only in the root cortex***

152 To gain insight into the tissue specificity of hydrotropism, we created a translational GFP
153 fusion to the *SnRK2.2* genomic sequence and expressed the reporter in the *snrk2.2 snrk2.3*
154 double mutant background. In the resulting lines, roots regained wild type sensitivity to 10
155 μ M ABA (Supplementary Fig. 4) and bent hydrotropically in the moisture gradient in air
156 assay (but not the split agar assay) (Supplementary Fig. 4). We assume that the differences
157 in hydrotropic response obtained using the different assays could be due to the moisture in
158 air gradient providing a steeper water potential gradient than the split agar assays. Hence,
159 the translational reporter appeared partially functional. Using confocal imaging SnRK2.2-
160 GFP signal was detected in nuclear and cytoplasmic compartments, consistent with the sub-
161 cellular localisation of its known regulatory targets^{24,25}. Moreover, at the tissue scale,
162 *SnRK2.2:SnRK2.2-GFP* was ubiquitously expressed throughout the root apex, including root
163 cap and elongation zone tissues (Fig. 2c).

164 To pinpoint the root tissue where SnRK2.2 is required during a hydrotropic response,
165 we expressed the *SnRK2.2* genomic sequence in the *snrk2.2 snrk2.3* double mutant
166 background using a suite of tissue- and zone-specific promoters. *SnRK2.2* expressed under
167 the control of the meristem and transition zone-specific *RCH1* promoter²⁶ complemented the
168 *snrk2.2 snrk2.3* hydrotropic defect (Fig. 2d). Surprisingly, rescue failed when *SnRK2.2* was
169 expressed specifically in the root cap (SOMBRERO²⁷, *SMB:SnRK2.2*), epidermis and lateral
170 root cap (WEREWOLF²⁸, *WER:SnRK2.2*), or endodermis (SCARECROW²⁹, *SCR:SnRK2.2*)
171 (Fig. 2d). In contrast, double mutant roots bent hydrotropically as the wild type when
172 expressing *SnRK2.2* in just the cortex (*Co2*³⁰, *Co2:SnRK2.2*) (Fig. 2d). *SnRK2.2* expression
173 levels in the *Co2:SnRK2.2* line were low in comparison to non-rescuing epidermal, lateral
174 root cap or endodermal driven lines, demonstrating that mutant rescue is not simply a dose
175 effect (Supplementary Fig. 5). In addition, we confirmed the hydrotropism response of the
176 *Co2:SnRK2.2* line using the moisture in air gradient assay (Supplementary Fig. 5). Hence,
177 root hydrotropism appears to require the ABA response machinery specifically in the cortex.

178

179 ***Cortex-specific MIZ1 expression rescues the miz1 hydrotropic defect***

180 To independently assess tissue specificity for the hydrotropic response, we determined
181 which tissues require MIZ1, a protein previously identified as essential for hydrotropism and
182 localized to cortex, epidermis, and lateral root cap¹⁸. We used various promoters to express
183 MIZ1-GFP in specific tissues in the *miz1* background (Supplementary Fig.6). When
184 constructs that included the *MIZ1* terminator were used, MIZ1-GFP expression driven by
185 *RCH1* was detected in the meristem, by *SMB* in the root cap, by *SCR* in the endodermis,
186 and by *COR* and by *Co2* in the cortex as expected^{26,27,29,31} (Supplementary Fig. 6).
187 Compared to *SCR* or *Co2*, the *COR* promoter drove MIZ1-GFP expression farther into the
188 elongation zone. In contrast, the *WER* promoter drove MIZ1-GFP expression not only in the
189 epidermis and lateral root cap, as expected²⁸, but also in the cortex. Like *COR*, expression
190 from *WER* continued well into the elongation zone. Note that none of these constructs
191 altered root growth rate appreciably (Supplementary Fig. 6).

192 Using the tissue-specific MIZ1-GFP constructs, we assayed hydrotropism using the
193 moisture gradient in air method that gave approximately 80° bending after 12 hours. As
194 expected, hydrotropic bending was fully rescued by expressing MIZ1-GFP under the *MIZ1*
195 promoter (Supplementary Fig. 6). In contrast, little or no hydrotropic curvature resulted when
196 MIZ1-GFP was expressed in root cap (*SMB*), in endodermis (*SCR*), or in the meristem
197 (*RCH1*). Mutant complementation was only partial using *Co2* to drive MIZ1-GFP expression,
198 but rescue was complete employing either *WER* or *COR* promoters, revealing a requirement
199 for MIZ1 in the elongation zone (Supplementary Fig. 6). Mutant rescue was also complete
200 when MIZ1-GFP expression was driven by the *PIN2* promoter, which like *WER*, drives
201 expression in lateral root cap, epidermis and cortex, which for the latter tissues continues
202 well into the elongation zone (Fig. 2 e-g). Finally, when *WER*-driven expression was
203 removed from the cortex, which happened if the native MIZ1 terminator was replaced by a
204 terminator from a heat-shock protein (HSP), *miz1* rescue essentially failed (Fig. 2e,g).
205 Identical responses for *WER*- and *PIN2*-driven MIZ1-GFP expression were obtained using
206 the split agar assay (Supplementary Fig. 5). Taken together, these results show that
207 hydrotropic bending requires MIZ1 expression specifically in the root cortex and that the
208 expression domain must span at least part of the elongation zone. This conclusion is
209 consistent with laser ablation and SnRK2.2 expression experiments that, when taken
210 collectively, questions the functional importance of root cap and meristem tissues during a
211 hydrotropic response.

212

213 ***Low levels of ABA promote root cell elongation***

214 Root cortical cells abut the endodermis (Fig. 2a), the recently reported site of ABA
215 accumulation in roots³². Hence, ABA response machinery in the cortex would be ideally
216 positioned to function like a ‘perimeter fence’, sensing any lateral movement of ABA from the
217 endodermis into outer root tissues, and presumably triggering growth responses. Whilst high
218 ABA levels inhibit root growth²³, low levels of this hormone are required to sustain root

219 elongation at low water potential³³⁻³⁵. To understand the ABA-dependent growth mechanism
220 underlying hydrotropism, we next investigated the effect of low doses of ABA on root growth.
221 Transferring seedlings onto 100 nM ABA stimulated root growth rate in the wild type but had
222 minimal effect on *snrk2.2 snrk2.3* (Fig. 3a, Supplementary Fig. 7). Comparing meristem and
223 elongation zone of those roots, 100 nM ABA appeared to change neither the length nor cell
224 number within the meristem but significantly increased elongation-zone length in wild type
225 and *Co2:SnRK2.2* complementation lines (Fig. 3c, Supplementary Fig. 7). The increased
226 root growth rate was accompanied by both an increased rate of cell production and an
227 increased mature cell length (Supplementary Fig. 7, Fig. 3b). Taken together, these data
228 suggest that low doses of ABA in these non-stressed plants stimulate rates of cell division
229 and elemental elongation.

230 As root hydrotropism represents an ABA-dependent differential growth response
231 (Fig. 2), we next addressed what size a hypothetical ABA gradient would have to be to drive
232 root bending. To calculate this, we first used image analysis to determine growth kinetics
233 during a hydrotropic response (Fig. 4a). Root tips bending in response to a water-potential
234 gradient initiated and maintained organ curvature in transition and elongation zones (Fig.
235 4b). Based on the observed growth promotion during the hydrotropic response, as well as on
236 the above results with 100 nM ABA, we calculated the minimum size of an ABA
237 concentration difference **between cortical cells on either side of the root** required for root
238 bending to be 4 nM (see Methods and Supplementary Note 1 for further details). Such a
239 small difference is effective because of the thinness of the root combined with the large size
240 of its elemental elongation rate. Detecting such a **hypothetical** ABA concentration difference
241 is currently beyond the limits of the hormone responsive reporters³⁶, helping to explain our
242 inability to detect changes in the hormone's tissue distribution following a hydrotropic
243 stimulus (Supplementary Fig. 8).

244

245 ***Hydrotropism is driven by differential cortical cell expansion***

246 Cells in the elongation zone, along with expanding anisotropically, also undergo a process
247 termed endoreplication (i.e. rounds of DNA replication without cell division)³⁷. To examine
248 tissue specificity in the promotion of root growth by ABA, we analysed nuclear ploidy of
249 specific tissues by performing cell sorting and DNA-content measurements. Significantly,
250 100 nM ABA stimulated endoreplication specifically in root cortical cells, as evidenced by the
251 increased fraction of 8C nuclei at the expense of 4C (Fig. 3e). In contrast, 100 nM ABA had
252 little if any effect on endoreplication in either atrichoblast or endodermal cells (Fig. 3d, f).
253 Hence, ABA appears to specifically trigger changes in cell cycle machinery in just the cortex,
254 consistent with our 'perimeter-fence' model.

255 One might question whether an asymmetry of growth-promoting mechanisms within
256 a single tissue could provide sufficient mechanical leverage to trigger root curvature. To
257 explore whether such changes in the dynamics of cortical cells are sufficient to drive root
258 bending during hydrotropism, we developed a mathematical model (see Methods and
259 Supplementary Note 1), taking advantage of recent theoretical work that successfully
260 recapitulates the root's growth rate profile by ascribing distinct mechanical contributions to
261 the various tissues³⁸. For a short period following exposure to the water potential gradient, a
262 small group of cortical cells on the dry side of the root were treated as undergoing early entry
263 into rapid elongation, changing their mechanical properties to be the same as cells in the
264 elongation zone. This differential elongation, coupled with the cell adhesion typical for plant
265 cells, caused the root midline to bend in this region. The predicted evolution of root tip angle,
266 and the curvature of the root midline, simulated bending at a similar rate to that observed
267 experimentally (Fig. 4c). Hence, asymmetric elongation in the root cortex appears to be a
268 plausible mechanism to drive hydrotropic bending. Taken together, these experimental data
269 and model simulations support our hypothesis that hydrotropism is driven by differential
270 cortical cell expansion.

271 If hydrotropic bending is driven by an asymmetric expansion of cortical cells in the
272 elongation zone, we reasoned that hydrotropism could be blocked by interfering with the
273 orderly progression of cells through the growth zone. To test this, we took advantage of the

274 overexpression phenotype of the cyclin-dependent kinase inhibitor SIAMESE (*SIM*), in which
275 cell division is inhibited and endoreplication is stimulated³⁹. We used a GAL4-VP16 driven
276 transactivation system to co-express *SIM* and a nuclear-localised GFP marker specifically in
277 either epidermis, cortex, or endodermis. In each case, root meristem cells overexpressing
278 *SIM* were enlarged (Fig. 5a-c) but cells in adjacent tissues were not detectably affected and
279 were of similar length to cells of roots expressing only the *GFP* marker (Fig. 5d-f). Next, we
280 tested each tissue-specific *SIM* over-expressing line for hydrotropism. Roots over-
281 expressing *SIM* in root epidermis or endodermis bent indistinguishably from the parental
282 lines, whereas *SIM* overexpression in the cortex blocked root hydrotropic bending (Fig. 5g).
283 In contrast, roots of every *SIM* overexpression line retained a wild-type response to gravity
284 (Fig. 5h), revealing that *SIM* overexpression in the cortex did not simply prevent all
285 differential root growth processes.

286

287 **Discussion**

288 We report that root tropic responses to gravity and water are driven by distinct molecular and
289 tissue-based mechanisms. In the case of gravity, root re-orientation is sensed by columella
290 cells at the root tip¹, triggering the formation of a lateral auxin gradient across the root with
291 higher concentrations on the lower side of the root^{40,41}. This auxin gradient is then
292 transported via the lateral root cap to the elongation zone³ where it elicits downward root
293 bending by stimulating elongation on the upper side and inhibiting elongation on the lower-
294 side⁴². In contrast, laser ablation experiments demonstrate here that neither meristem,
295 lateral root cap nor columella cells are required to perceive a water potential gradient (Fig.
296 1). Hence, unlike its role in root gravitropism, the elongation zone performs a dual function
297 during a hydrotropic response both to sense a water potential gradient and subsequently
298 undergo differential growth.

299 We also confirm that root hydrotropism employs the hormone ABA and that the ABA
300 signal transduction components SnRK2.2 and SnRK2.3 play a key role regulating root re-

301 orientation. Surprisingly, targeted *SnRK2.2* expression studies in *snrk2.2 snrk2.3* (Fig. 2)
302 revealed the critical importance during hydrotropism of ABA response machinery just in the
303 cortex. The importance of this specific root tissue for hydrotropism was further supported by
304 the response depending on cortical expression of *MIZ1* (Fig. 2). Taken together, our results
305 demonstrate that ABA and *MIZ1* responses in the cortex of the root elongation zone play a
306 central role in hydrotropic response of *A. thaliana* roots (Fig. 6). Hence, root gravitropic and
307 hydrotropic responses are driven by distinct signals and tissue-based mechanisms.
308 Consistent with our conclusion, Krieger *et al.*⁴³ recently described the opposing effect of
309 ROS on these tropic responses and the distinct positions at which roots bend during
310 gravitropic and hydrotropic responses.

311 A key question for hydrotropic research is to understand how a modest gradient in
312 water potential across the root is perceived (and presumably amplified) into a growth
313 response. Mechanosensing, differential movement of water, ions or signalling molecules all
314 represent likely candidates⁴⁴. In the case of ABA, localisation of its biosynthesis genes in the
315 vasculature⁴⁵, endodermal localisation of its accumulation in roots³² and our mapping of ABA
316 response to the adjacent cortical tissue leads us to propose a 'perimeter fence model' (Fig.
317 6). We **hypothesise** that roots regulate hydrotropism by linking asymmetric ABA distribution
318 with differential water uptake into the root elongation zone. Differential water movement
319 **could** carry ABA from inner tissues to cortical cells (on the low water potential side) or away
320 from cortical cells towards the stele (on the high water potential side) as described in other
321 plant species⁴⁶. The resulting radial ABA concentration difference **could then** promote
322 differential cortical expansion, triggering the root to re-orient its growth direction towards a
323 source of higher water potential. **Testing of this hypothesis awaits the development of ABA**
324 **sensors/detection methods more sensitive than those currently available.**

325

326 **METHODS**

327 **Ablation of root-tip cells using laser-microscopy systems**

328 For micro-beam laser irradiation, 4-day-old seedlings were aligned in a micro-chamber
329 comprising two glass coverslips (25×60 mm² and 24×24 mm², Matsunami) and a seal
330 (TaKaRa Slide Seal for in situ PCR, Takara Bio). The micro-chamber was filled with low-
331 melting agar (half-strength MS medium, 0.4% (w/v) sucrose [Wako Pure Chemical
332 Industries], 0.2% (w/v) low-melting agarose [SeaPlaque; FMC BioProducts]). These samples
333 were put on the stage of a microscope (Nikon ECLIPSE TiE, Nikon) and irradiated with a N₂
334 pulsed micro-beam laser through Coumarin 440 with an averaged power of 330 kW for a 3
335 to 5 nanosecond pulse (MicroPoint PIJ-3-1; Andor Technology). For femtosecond laser
336 irradiation, seedlings were placed on the half-strength MS medium on a glass slide.
337 Amplified femtosecond laser pulses from a re-generatively amplified Ti:sapphire
338 femtosecond laser system (IFRIT; 780 ± 5 nm, 230 fs, < 1 mJ/pulse, 1 kHz, Cyber Laser
339 Inc.) were focused onto root cap cells through a 10x objective lens (UPlanSApo NA 0.4,
340 Olympus) on a confocal laser scanning microscope (FV1000-BX51, Olympus). Laser pulses
341 (200) were detected with a mechanical shutter (gate time: 200 ms) and delivered to the
342 sample. The laser pulse was collimated by dual convex lenses before the microscope, and
343 the laser focal point was tuned to the plane of the image. The diameter of the laser focal
344 point, which is consistent with the beam waist, was about 1 μm. A neutral density filter was
345 put between the laser and microscope and used to tune the laser pulse energy to around
346 400 nJ/pulse, which is about 4 times larger than the threshold energy for cavitation bubble
347 generation in water (100 nJ/pulse). Laser-ablated seedlings were incubated on half-strength
348 MS medium for 1 h in a vertical position before performing further assays.

349

350 **Root tropism and growth assays**

351 The hydrotropism assay shown in Fig. 1 and Supplementary Fig. 5b-e were performed as
352 described previously using a split-agar system with 812 mM sorbitol¹¹. Gravitropism assays
353 shown in Fig. 1 and Supplementary Fig. 2 were performed using 1% agar medium with or
354 without 0.5x MS medium as described previously¹⁶. Hydrotropism assays shown in Fig. 2g
355 and Supplementary Fig. 2g-r, 4e-f, 5 f-g and 6 were performed using a moisture gradient in

356 air as described previously¹¹. Four-day-old seedlings were used for all tropism assays
357 described above.

358 Hydrotropism assays shown in Fig. 2b and d, 4 and 5 and Supplementary Fig. 2s, 3, 4d and
359 8 were performed as previously described⁴⁷ using 5-day-old seedlings in a split-agar system
360 with 400 mM sorbitol.

361 For gravitropism assays shown in Fig. 5, 5-day-old seedlings were transferred to new plates
362 containing 0.5x MS medium with 1% agar. After acclimatisation for 2 hours in the controlled
363 environment room, plates were rotated by 90°. Images of seedlings were acquired using an
364 automated imaging platform⁴⁸ and root tip angle and length determined using the Fiji image
365 processing package (<http://fiji.sc/Fiji>).

366 For assessing root growth response to ABA, 5-day-old seedlings were transferred to new
367 plates containing 0.5x MS medium with the indicated amount of ABA (Sigma). To determine
368 meristem cell number and length, longitudinal images of root tips clearly showing the cortex
369 cell file were taken with a confocal laser scanning microscope, using propidium iodide to
370 stain cell walls. Starting from the QC, the length of individual cortex cells was determined
371 using the Cell-o-Tape macro⁴⁹ for Fiji. The mean length of meristem cells was calculated
372 using ten cells from the rapid amplifying region of the meristem (cells 10-19 counting
373 shootward from the QC), and the end of the meristem deemed to have been reached when
374 consecutive cells had reached and/or exceeded the mean length by two. Cell production
375 rates were calculated as previously described⁵⁰.

376

377 **Modelling ABA and water potential gradients**

378 Changes in growth rate under the addition of 100 nM ABA (Fig. 3a) and measurements of
379 root tip angle change (Fig. 2b) were used to estimate required differences in ABA
380 concentration between the cortical cells on the wet and dry side of the root.

381 From geometrical considerations (see Supplementary Note 1, Section 1 for further details),
382 the difference in growth rates between the cortical cells on the wet and dry side of the root
383 needed to generate the observed rate of change of tip angle over the first hour of the

384 hydrotropism assay was calculated. Under the assumption that the effect of ABA on growth
385 is linear in the concentration range from 0 to 100 nM, the necessary difference in ABA
386 concentration between cortical cells on the wet and dry sides was calculated to be 4 nM.

387

388 The water potential gradient experienced by the root was estimated by the solution of the
389 diffusion equation for sorbitol in agar, combined with the van 't Hoff equation which relates
390 water potential and solute concentration. From the geometry of the hydrotropism assay,
391 away from the edges of the agar plate, the resulting water potential distribution can be
392 treated as a function purely of the distance from the cut, namely

$$\Phi = -A \operatorname{erfc}\left(\frac{x}{2\sqrt{Dt}}\right)$$

393 Here x is distance from the cut, t is time after sorbitol is added to the plate, $D = 10^{-5} \text{ cm}^2/\text{hr}$
394 and $A = 1 \text{ MPa}$. Using the distance of the initial placement of the root tip from the cut (2.5
395 mm) as an estimate of the distance of the root centre line from the cut and $100 \mu\text{m}$ as an
396 estimate of the root diameter, the relative difference in water potential across the root was
397 estimated through the evaluation of the water potential distribution at $x = 2.5 \pm 0.05 \text{ mm}$.

398

399 **Modelling root bending**

400 A mechanical model has been developed to describe hydrotropism-associated root bending.
401 The approach³⁸ exploits the large aspect ratio of the root, which allows a relatively simple
402 description of bending in terms of the stretch and curvature of the root midline. A viscoplastic
403 constitutive relation is adopted (viscous flow where the yield stress is exceeded), with the
404 yield stress of cortical cells on the dry side of the root modified in response to a hydrotropic
405 stimulus; the resulting partial differential equations for the dependence of midline stretch and
406 curvature in terms of time and arc length are solved numerically by a finite-difference
407 approach. Further details are given in the Supplementary Note 1, Section 2.

408

409 *Note: Supplementary Information (Supplementary Methods, Supplementary Figures and two*
410 *Supplementary Notes) is available in the online version of the paper.*

411

412 **References**

413

- 414 1 Blancaflor, E. B., Fasano, J. M. & Gilroy, S. Mapping the functional roles of cap cells in the
415 response of Arabidopsis primary roots to gravity. *Plant physiology* **116**, 213-222 (1998).
- 416 2 Ottenschlager, I. *et al.* Gravity-regulated differential auxin transport from columella to
417 lateral root cap cells. *Proceedings of the National Academy of Sciences of the United States*
418 *of America* **100**, 2987-2991, doi:10.1073/pnas.0437936100 (2003).
- 419 3 Swarup, R. *et al.* Root gravitropism requires lateral root cap and epidermal cells for transport
420 and response to a mobile auxin signal. *Nature cell biology* **7**, 1057-1065,
421 doi:10.1038/ncb1316 (2005).
- 422 4 Rahman, A. *et al.* Gravitropism of Arabidopsis thaliana roots requires the polarization of
423 PIN2 toward the root tip in meristematic cortical cells. *The Plant cell* **22**, 1762-1776,
424 doi:10.1105/tpc.110.075317 (2010).
- 425 5 Friml, J. Subcellular trafficking of PIN auxin efflux carriers in auxin transport. *European*
426 *journal of cell biology* **89**, 231-235, doi:10.1016/j.ejcb.2009.11.003 (2010).
- 427 6 Jaffe, M. J., Takahashi, H. & Biro, R. L. A pea mutant for the study of hydrotropism in roots.
428 *Science* **230**, 445-447, doi:10.1126/science.230.4724.445 (1985).
- 429 7 Takahashi, H. & Suge, H. Root Hydrotropism of an Agravitropic Pea Mutant, Ageotropum.
430 *Physiol Plantarum* **82**, 24-31 (1991).
- 431 8 Takahashi, H. & Scott, T. K. Intensity of Hydrostimulation for the Induction of Root
432 Hydrotropism and Its Sensing by the Root Cap. *Plant Cell and Environment* **16**, 99-103,
433 doi:DOI 10.1111/j.1365-3040.1993.tb00850.x (1993).
- 434 9 Miyazawa, Y. *et al.* Effects of locally targeted heavy-ion and laser microbeam on root
435 hydrotropism in Arabidopsis thaliana. *Journal of radiation research* **49**, 373-379 (2008).
- 436 10 Miyamoto, N., Ookawa, T., Takahashi, H. & Hirasawa, T. Water uptake and hydraulic
437 properties of elongating cells in hydrotropically bending roots of Pisum sativum L. *Plant &*
438 *cell physiology* **43**, 393-401 (2002).
- 439 11 Kaneyasu, T. *et al.* Auxin response, but not its polar transport, plays a role in hydrotropism of
440 Arabidopsis roots. *Journal of experimental botany* **58**, 1143-1150, doi:10.1093/jxb/erl274
441 (2007).
- 442 12 Takahashi, N., Goto, N., Okada, K. & Takahashi, H. Hydrotropism in abscisic acid, wavy, and
443 gravitropic mutants of Arabidopsis thaliana. *Planta* **216**, 203-211, doi:10.1007/s00425-002-
444 0840-3 (2002).
- 445 13 Takahashi, H., Miyazawa, Y. & Fujii, N. Hormonal interactions during root tropic growth:
446 hydrotropism versus gravitropism. *Plant molecular biology* **69**, 489-502,
447 doi:10.1007/s11103-008-9438-x (2009).
- 448 14 Shkolnik, D., Krieger, G., Nuriel, R. & Fromm, H. Hydrotropism: Root Bending Does Not
449 Require Auxin Redistribution. *Mol Plant* **9**, 757-759, doi:10.1016/j.molp.2016.02.001 (2016).
- 450 15 Antoni, R. *et al.* PYRABACTIN RESISTANCE1-LIKE8 Plays an Important Role for the Regulation
451 of Abscisic Acid Signaling in Root. *Plant physiology* **161**, 931-941, doi:10.1104/pp.112.208678
452 (2013).
- 453 16 Kobayashi, A. *et al.* A gene essential for hydrotropism in roots. *Proceedings of the National*
454 *Academy of Sciences of the United States of America* **104**, 4724-4729,
455 doi:10.1073/pnas.0609929104 (2007).
- 456 17 Moriwaki, T., Miyazawa, Y., Fujii, N. & Takahashi, H. Light and abscisic acid signalling are
457 integrated by MIZ1 gene expression and regulate hydrotropic response in roots of

458 Arabidopsis thaliana. *Plant Cell and Environment* **35**, 1359-1368, doi:10.1111/j.1365-
459 3040.2012.02493.x (2012).

460 18 Moriwaki, T., Miyazawa, Y., Kobayashi, A. & Takahashi, H. Molecular mechanisms of
461 hydrotropism in seedling roots of Arabidopsis thaliana (Brassicaceae). *Am J Bot* **100**, 25-34,
462 doi:10.3732/ajb.1200419 (2013).

463 19 Cutler, S. R., Rodriguez, P. L., Finkelstein, R. R. & Abrams, S. R. Abscisic Acid: Emergence of a
464 Core Signaling Network. *Annu Rev Plant Biol* **61**, 651-679, doi:10.1146/annurev-arplant-
465 042809-112122 (2010).

466 20 Ma, Y. *et al.* Regulators of PP2C Phosphatase Activity Function as Abscisic Acid Sensors.
467 *Science* **324**, 1064-1068, doi:10.1126/science.1172408 (2009).

468 21 Park, S. Y. *et al.* Abscisic Acid Inhibits Type 2C Protein Phosphatases via the PYR/PYL Family
469 of START Proteins. *Science* **324**, 1068-1071, doi:10.1126/science.1173041 (2009).

470 22 Fujii, H. *et al.* In vitro reconstitution of an abscisic acid signalling pathway. *Nature* **462**, 660-
471 U138, doi:10.1038/nature08599 (2009).

472 23 Fujii, H., Verslues, P. E. & Zhu, J. K. Identification of two protein kinases required for abscisic
473 acid regulation of seed germination, root growth, and gene expression in Arabidopsis. *The*
474 *Plant cell* **19**, 485-494, doi:10.1105/tpc.106.048538 (2007).

475 24 Kline, K. G., Barrett-Wilt, G. A. & Sussman, M. R. In planta changes in protein
476 phosphorylation induced by the plant hormone abscisic acid. *Proceedings of the National*
477 *Academy of Sciences of the United States of America* **107**, 15986-15991,
478 doi:10.1073/pnas.1007879107 (2010).

479 25 Wang, P. *et al.* Quantitative phosphoproteomics identifies SnRK2 protein kinase substrates
480 and reveals the effectors of abscisic acid action. *Proceedings of the National Academy of*
481 *Sciences of the United States of America* **110**, 11205-11210, doi:10.1073/pnas.1308974110
482 (2013).

483 26 Casamitjana-Martinez, E. *et al.* Root-specific CLE19 overexpression and the sol1/2
484 suppressors implicate a CLV-like pathway in the control of Arabidopsis root meristem
485 maintenance. *Current biology : CB* **13**, 1435-1441 (2003).

486 27 Willemsen, V. *et al.* The NAC domain transcription factors FEZ and SOMBRERO control the
487 orientation of cell division plane in Arabidopsis root stem cells. *Developmental cell* **15**, 913-
488 922, doi:10.1016/j.devcel.2008.09.019 (2008).

489 28 Lee, M. M. & Schiefelbein, J. WEREWOLF, a MYB-related protein in Arabidopsis, is a position-
490 dependent regulator of epidermal cell patterning. *Cell* **99**, 473-483 (1999).

491 29 Wysocka-Diller, J. W., Helariutta, Y., Fukaki, H., Malamy, J. E. & Benfey, P. N. Molecular
492 analysis of SCARECROW function reveals a radial patterning mechanism common to root and
493 shoot. *Development* **127**, 595-603 (2000).

494 30 Heidstra, R., Welch, D. & Scheres, B. Mosaic analyses using marked activation and deletion
495 clones dissect Arabidopsis SCARECROW action in asymmetric cell division. *Genes &*
496 *development* **18**, 1964-1969, doi:10.1101/gad.305504 (2004).

497 31 Lee, J. Y. *et al.* Transcriptional and posttranscriptional regulation of transcription factor
498 expression in Arabidopsis roots. *Proceedings of the National Academy of Sciences of the*
499 *United States of America* **103**, 6055-6060, doi:10.1073/pnas.0510607103 (2006).

500 32 Ondzighi-Assoume, C. A., Chakraborty, S. & Harris, J. M. Environmental Nitrate Stimulates
501 Abscisic Acid Accumulation in Arabidopsis Root Tips by Releasing It from Inactive Stores. *The*
502 *Plant cell* **28**, 729-745, doi:10.1105/tpc.15.00946 (2016).

503 33 Sharp, R. E., Wu, Y. J., Voetberg, G. S., Saab, I. N. & Lenoble, M. E. Confirmation That
504 Abscisic-Acid Accumulation Is Required for Maize Primary Root Elongation at Low Water
505 Potentials. *Journal of experimental botany* **45**, 1743-1751 (1994).

506 34 Xu, W. F. *et al.* Abscisic acid accumulation modulates auxin transport in the root tip to
507 enhance proton secretion for maintaining root growth under moderate water stress. *New*
508 *Phytologist* **197**, 139-150, doi:10.1111/nph.12004 (2013).

- 509 35 Rowe, J. H., Topping, J. F., Liu, J. & Lindsey, K. Abscisic acid regulates root growth under
510 osmotic stress conditions via an interacting hormonal network with cytokinin, ethylene and
511 auxin. *The New phytologist*, doi:10.1111/nph.13882 (2016).
- 512 36 Waadt, R., Hsu, P. K. & Schroeder, J. I. Abscisic acid and other plant hormones: Methods to
513 visualize distribution and signaling. *Bioessays* **37**, 1338-1349, doi:10.1002/bies.201500115
514 (2015).
- 515 37 De Veylder, L., Larkin, J. C. & Schnittger, A. Molecular control and function of
516 endoreplication in development and physiology. *Trends in plant science* **16**, 624-634,
517 doi:10.1016/j.tplants.2011.07.001 (2011).
- 518 38 Dyson, R. J. *et al.* Mechanical modelling quantifies the functional importance of outer tissue
519 layers during root elongation and bending. *The New phytologist* **202**, 1212-1222,
520 doi:10.1111/nph.12764 (2014).
- 521 39 Churchman, M. L. *et al.* SIAMESE, a plant-specific cell cycle regulator, controls
522 endoreplication onset in Arabidopsis thaliana. *The Plant cell* **18**, 3145-3157,
523 doi:10.1105/tpc.106.044834 (2006).
- 524 40 Brunoud, G. *et al.* A novel sensor to map auxin response and distribution at high spatio-
525 temporal resolution. *Nature* **482**, 103-106, doi:10.1038/nature10791 (2012).
- 526 41 Band, L. R. *et al.* Root gravitropism is regulated by a transient lateral auxin gradient
527 controlled by a tipping-point mechanism. *Proceedings of the National Academy of Sciences*
528 *of the United States of America* **109**, 4668-4673, doi:10.1073/pnas.1201498109 (2012).
- 529 42 Mullen, J. L., Ishikawa, H. & Evans, M. L. Analysis of changes in relative elemental growth
530 rate patterns in the elongation zone of Arabidopsis roots upon gravistimulation. *Planta* **206**,
531 598-603, doi:DOI 10.1007/s004250050437 (1998).
- 532 43 Krieger, G., Shkolnik, D., Miller, G. & Fromm, H. Reactive oxygen species tune root tropic
533 responses. *Plant physiology*, doi:10.1104/pp.16.00660 (2016).
- 534 44 Shkolnik, D. F., H. The Cholodny-Went theory does not explain hydrotropism. *Plant Sci* **252**,
535 400-403 (2016).
- 536 45 Nambara, E. & Marion-Poll, A. Abscisic acid biosynthesis and catabolism. *Annu Rev Plant Biol*
537 **56**, 165-185, doi:10.1146/annurev.arplant.56.032604.144046 (2005).
- 538 46 Freundl, E., Steudle, E. & Hartung, W. Water uptake by roots of maize and sunflower affects
539 the radial transport of abscisic acid and its concentration in the xylem. *Planta* **207**, 8-19,
540 doi:DOI 10.1007/s004250050450 (1998).
- 541 47 Antoni, R., Dietrich, D., Bennett, M. J. & Rodriguez, P. L. Hydrotropism: Analysis of the Root
542 Response to a Moisture Gradient. *Methods in molecular biology* **1398**, 3-9, doi:10.1007/978-
543 1-4939-3356-3_1 (2016).
- 544 48 Wells, D. M. *et al.* Recovering the dynamics of root growth and development using novel
545 image acquisition and analysis methods. *Philosophical transactions of the Royal Society of*
546 *London. Series B, Biological sciences* **367**, 1517-1524, doi:10.1098/rstb.2011.0291 (2012).
- 547 49 French, A. P. *et al.* Identifying biological landmarks using a novel cell measuring image
548 analysis tool: Cell-o-Tape. *Plant methods* **8**, 7, doi:10.1186/1746-4811-8-7 (2012).
- 549 50 Baskin, T. I. Patterns of root growth acclimation: constant processes, changing boundaries.
550 *Wiley interdisciplinary reviews. Developmental biology* **2**, 65-73, doi:10.1002/wdev.94
551 (2013).

554 ACKNOWLEDGEMENTS

555 The authors thank Caroline Howells, Kamal Swarup and Morag Whitworth for technical
556 assistance, Jian-Kang Zhu for providing *snrk2.2 snrk2.3* seeds, Wim Grunewald for pDONR-
557 L1-GAL4-VP16-R2, Sumika Tsukinoki for generating *WER:MIZ1-GFP(HSPter)* and

558 *PIN2:MIZ1-GFP(HSPter)* transgenic plants and acknowledge the following funding agencies
559 for financial support: D.D., J.F., R.A., D.W., S.T., C.S., S.M., M.R.O., L.R.B., R.D., O.J., J.K.,
560 J.R., T.B. and M.J.B. thank the Biological and Biotechnology Science Research Council
561 (BBSRC) for responsive mode and CISB awards to the Centre for Plant Integrative Biology;
562 D.W., C.S., S.M., M.R.O., J.K., T.P. and M.J.B. thank the European Research Council (ERC)
563 for FUTUREROOTS project funding; L.R.B. thanks the Leverhulme Trust for an Early Career
564 Fellowship; V.B., R.B. and L.D.V are supported by grants of the Research Foundation
565 Flanders (G.002911N). R.B. and M.J.B. thank the Royal Society for Newton and Wolfson
566 Research Fellowship awards; R.A., T.I.B. and M.J.B. thank the FP7 Marie-Curie Fellowship
567 Scheme; J.D. and M.J.B. thank the GII scheme; and V.B., R.B., L.D.V. and M.J.B. thank the
568 Interuniversity Attraction Poles Programme (IUAP P7/29 "MARS"), initiated by the Belgian
569 Science Policy Office. R.B.P was funded by grants from the Knut and Alice Wallenberg
570 Foundation. This work was also supported by a Grant-in-Aid for Scientific Research on
571 Innovative Areas (No. 24620002) from the Ministry of Education, Culture, Sports, Science
572 and Technology (MEXT) of Japan to H.T., a Grant-in-Aid for Young Scientists (B) (No.
573 26870057) from the Japan Society for the Promotion of Science (JSPS) to A.K., and the
574 Funding Program for Next-Generation World-Leading Researchers (GS002) to Y.M. L.P.
575 was financially supported by a scholarship from the Japanese government. T.-W.B. was
576 financially supported by the Funding Program for Next-Generation World-Leading
577 Researchers (GS002) and the Grant-in-Aid for Scientific Research on Innovative Areas (No.
578 24620002).

579

580 **AUTHOR CONTRIBUTIONS**

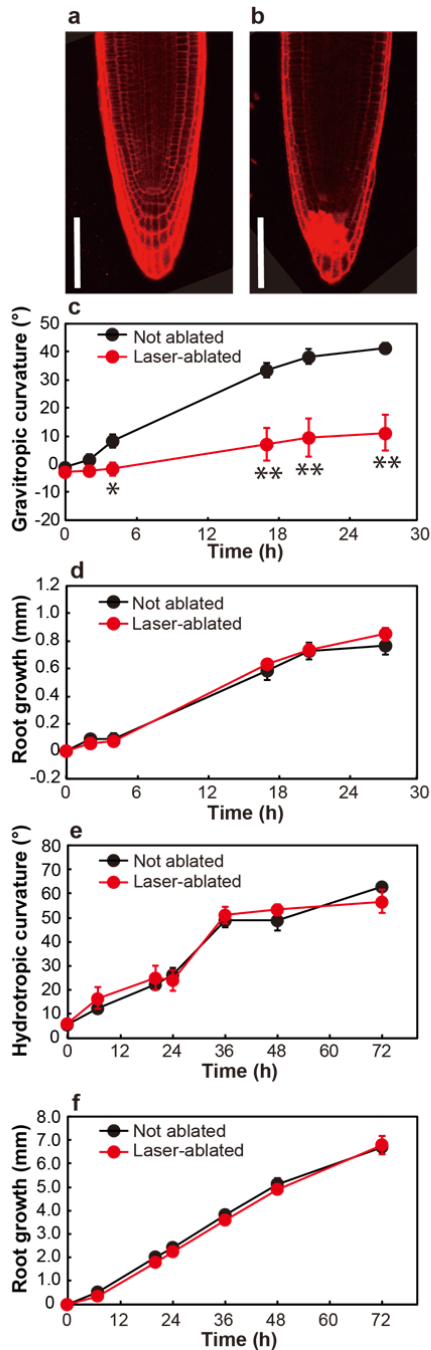
581 D.D., L.P., A.K., J.F., V.B., R.B., R.A., T.N., S.H., T.-W.B., Y.M., D.M.W., S.T., C.J.S.
582 performed experimental work and data analysis and mathematical modelling. D.M.W.,
583 M.R.O., L.R.B., R.D., O.J., J.R.K., S.J.M., J.R., R.B., J.D., P.L.R., T.I.B., T.P., L.D.V., N.F.,
584 Y.M., A.N., Y.H., H.T. and M.J.B. oversaw project planning and discussed experimental
585 results and modelling simulations. D.D., L.P., A.K., N.F., Y.M., T.I.B., H.T. and M.J.B. wrote
586 the paper.

587

588 **COMPETING FINANCIAL INTERESTS**

589 The authors declare no competing financial interests.

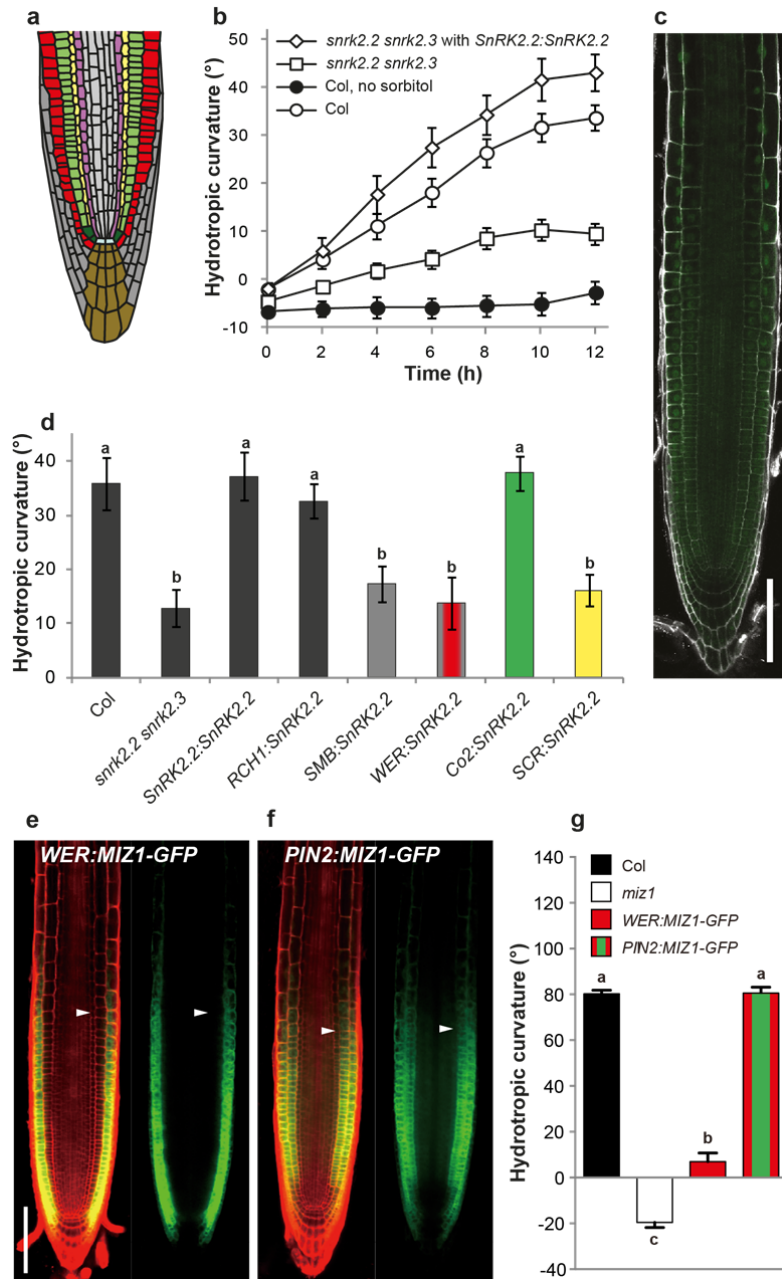
590



592

593 **Figure 1 Laser ablation of columella cells affects the gravitropic but not the hydrotropic**
 594 **response of roots**

595 Confocal fluorescence micrograph of propidium iodide-stained primary root tips before (a) and after
 596 (b) femtosecond-laser ablation of the columella, scale bar = 100 μm . Time-course study of root
 597 gravitropic curvature (c) and root growth (d). In c, 0° equals horizontal. Time-course study of root
 598 hydrotropic curvature (e) and root growth (f). In e, 0° equals vertical. The hydrotropism assay was
 599 performed using the split agar system with 812 mM sorbitol. Values are mean \pm SEM of a
 600 representative experiment, $n = 3 - 6$, from three independent experiments. Asterisks indicate
 601 statistically significant differences ($*p < 0.05$, $**p < 0.01$, Student's t -test).



602

603 **Figure 2 ABA signalling in the cortex is crucial for root hydrotropism**

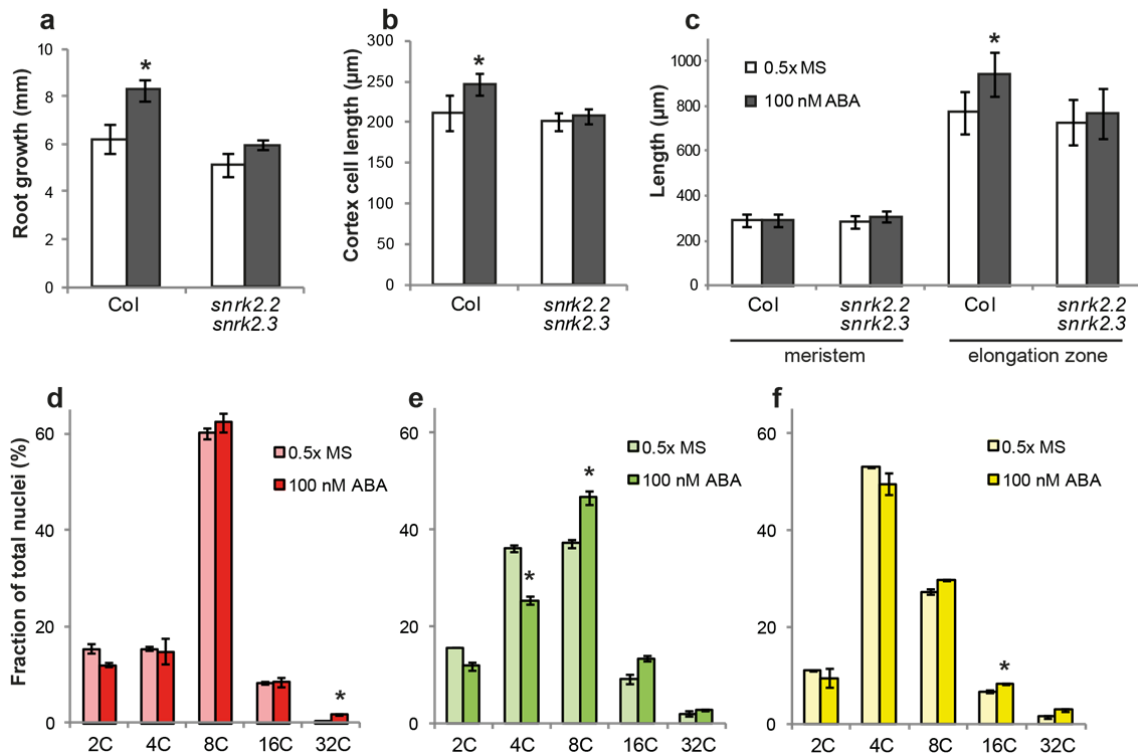
604 **a** Schematic drawing indicating tissues in the root tip, grey: lateral root cap, red: epidermis, green:
 605 cortex, yellow: endodermis. **b** Kinetics of hydrotropic curvature after transferring seedlings to split
 606 agar plates with 400 mM sorbitol. Values are mean ± SEM, $n = 29 - 40$. **c** Expression of
 607 *SnRK2.2:SnRK2.2-GFP* in the root tip, scale bar = 100 μm. **d** Hydrotropic curvature 12 h after transfer
 608 to split agar plates with 400 mM sorbitol. Values are mean ± SEM, $n = 24-31$. Different letters indicate
 609 statistically significant differences ($p < 0.05$, Fisher's LSD). **e**, **f** Expression pattern of MIZ1-GFP
 610 fusion protein under control of (e) the *WER* and (f) *PIN2* promoters with *HSP* terminator. Left-hand
 611 image shows an over lay of fluorescence from GFP (green) and PI (red), right-hand image shows
 612 GFP only. Arrowhead indicates the approximate rootward boundary of the elongation zone, scale bar
 613 = 100 μm. **g** Hydrotropic curvature 12 h after transfer of seedlings to the moisture gradient in air assay
 614 system. Values are mean ± SEM of three independent experiments, $n = 35-44$. Different letters
 615 indicate statistically significant differences ($p < 0.05$, Tukey HSD test).

616

617

618

619



620

621

622 **Figure 3 Root growth and cortical endoreplication are induced by low levels of ABA**

623 **a – c** Root growth and histology. **a** Root growth without (0.5x MS) or with 100 nM ABA 24 h after
624 transfer. Values are mean of three experiments \pm SD, $n = 12-40$. **b, c** Seedlings treated as in (a) were
625 stained with propidium iodide and images taken with a confocal microscope. **b** Cell length of mature
626 cortex cells. Values are mean \pm SD, $n = 18-47$ cells for 10 roots per line and treatment. **c** Meristem
627 length was determined using Cell-o-Tape and an arithmetic method to determine the meristem end.
628 Elongation zone length was determined by measuring the distance from the end of the lateral root cap
629 until the first root hair bulge. Values are mean \pm SD, $n = 11-28$. For a - c: * statistically significant
630 different ($p < 0.01$, Student's t -test). **e – f** Endoreplication. DNA content of nuclei isolated from (d) the
631 epidermis (non-hair cells), (e) cortex and (f) endodermis of roots treated for 24 h without (0.5x MS,
632 light bars) or with 100nM ABA (dark bars). Values are mean \pm SD. For d - f: * statistically significant
633 different ($p < 0.05$, Student's t -test).

634

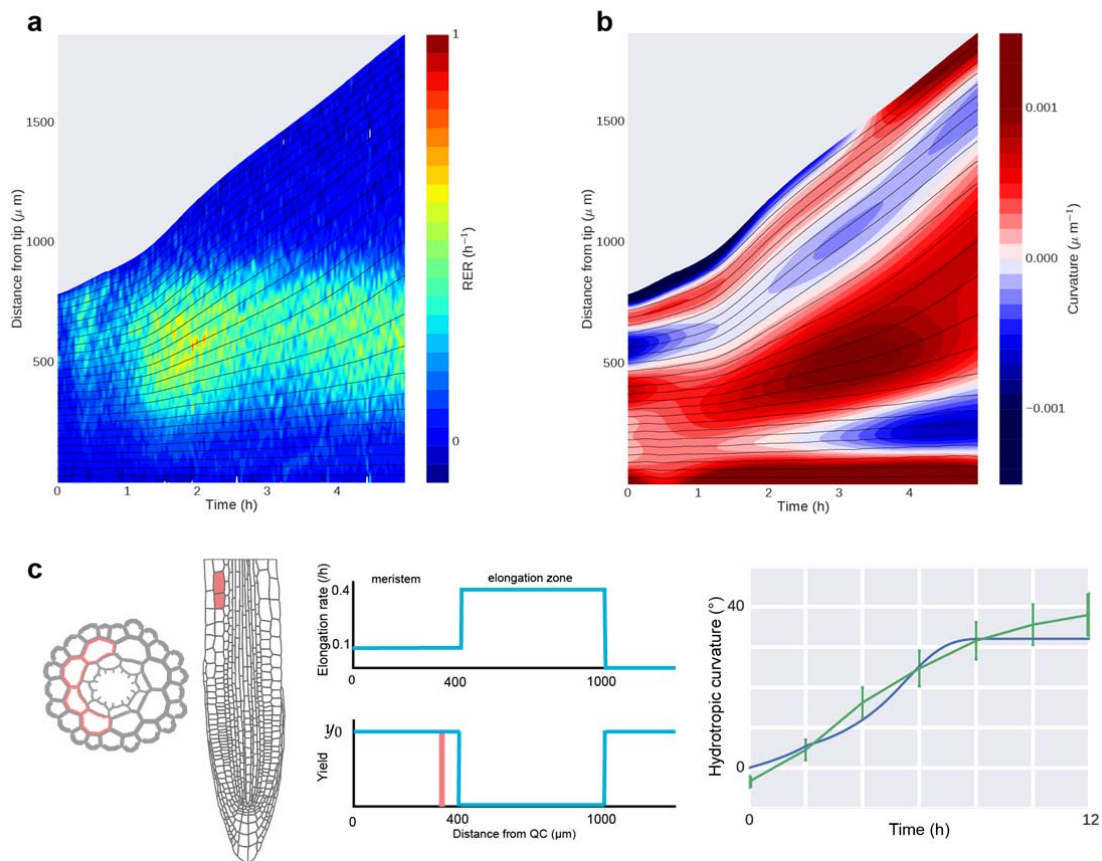
635

636

637

638

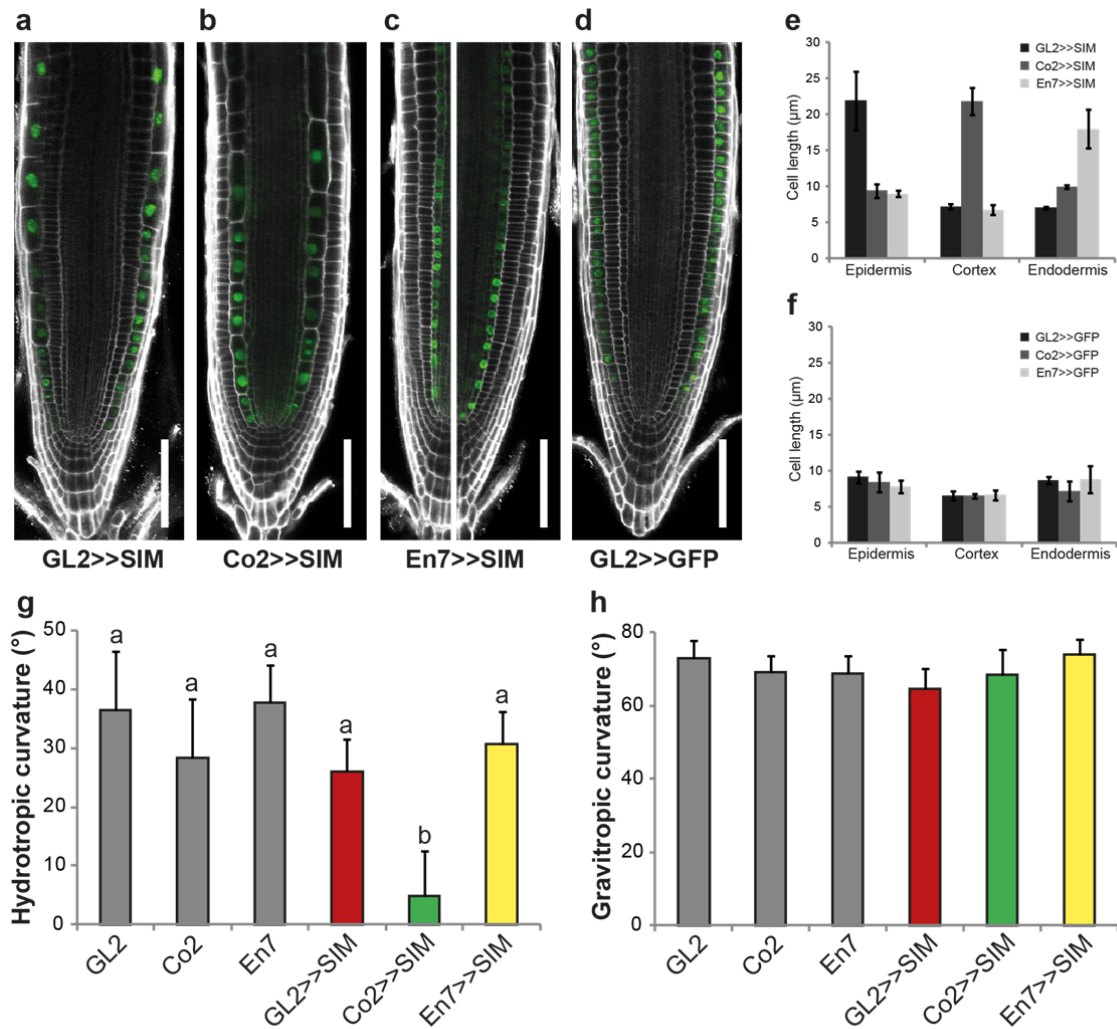
639
640
641
642
643



644
645
646
647
648
649
650
651
652
653
654
655
656
657
658

Figure 4 Changes in root growth in response to hydrotropism

a Relative elongation rate and **b** curvature of a hydrotropically bending root during the first 5 h after transfer to a split agar plate with 400 mM sorbitol. Solid lines show the trajectories of points equally spaced at time zero. Representative data from four independent repeats shown. **c** Modelling the hydrotropism response: The transition between the meristem and elongation zone is marked by a drop in yield stress leading to a rise in elongation rate (centre); the large yield stress y_0 in the meristem inhibits cell expansion; cortical cells on the dry side of the root (pink in transverse and axial cross-sections, left) enter elongation early for the first 2 h, with asymmetric softening across the root generating a bend. Simulated (blue) and experimental (green) hydrotropic curvature profiles are compared (right).

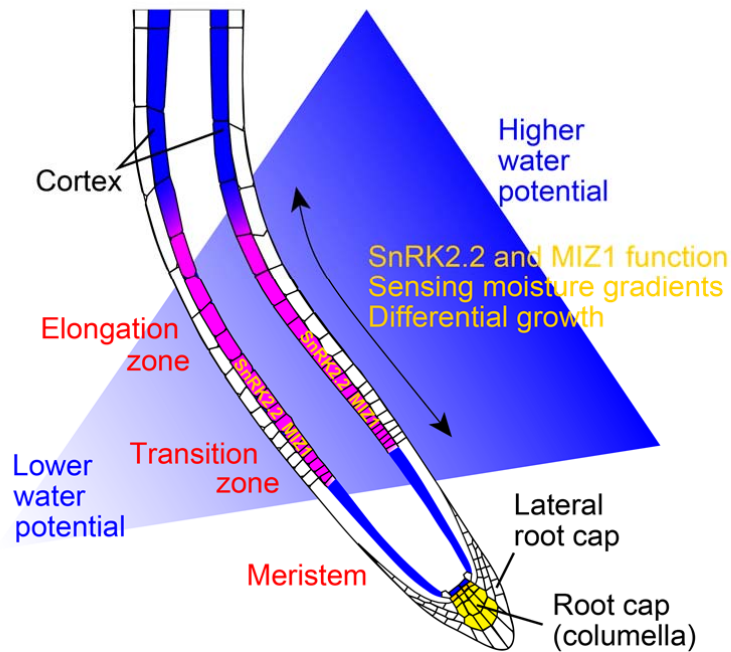


659

660 **Figure 5 Inhibition of differential cell elongation in the cortex prevents hydrotropism but not**
 661 **gravitropism**

662 **a – d** Confocal images of root tips co-expressing *SIM* and *NLS-GFP* (green) in (a) epidermis, (b)
 663 cortex, (c) endodermis, or (d) expressing *NLS-GFP* in epidermis. Cell walls were stained with
 664 propidium iodide (white). In c, two images of the same root are shown, for better visualization of the
 665 endodermis cell file. Scale bars for a - d = 100 μm . **e, f** Quantification of cell lengths for epidermis,
 666 cortex and endodermis files in the meristem. Values are mean \pm SD, $n = 7$ -52 cells from three plants
 667 for each line and tissue. **g** Hydrotropic curvature 10 h after transfer to split agar plates with 400 mM
 668 sorbitol. Values are mean \pm 2x SEM, $n = 14$ -15 for parental lines (GL2, Co2, En7) and $n = 56$ for *SIM*
 669 expression lines (GL2>>SIM, Co2>>SIM, En7>>SIM). Different letters indicate statistically significant
 670 differences ($p < 0.05$, Fisher's LSD). **h** Gravitropic curvature 8 h after plates were rotated by 90 $^{\circ}$.
 671 Values are mean \pm 2x SEM, $n = 30$ -31.

672



673

674 **Figure 6 Conceptual model for root hydrotropism**

675 SnRK2.2 and MIZ1 expression in cortex cells of the transition and elongation zone are required to
 676 mediate the ABA-dependent differential growth response to a water potential gradient. Perception of
 677 the water potential gradient does not require tissues in the root cap or meristem, but takes place in
 678 the transition and elongation zones where the differential growth response occurs.

679

680

681

682